IEEE Access
Multidisciplinary | Rapid Review | Open Access Journal

Received May 16, 2019, accepted June 10, 2019, date of publication June 27, 2019, date of current version July 18, 2019.

Digital Object Identifier 10.1109/ACCESS.2019.2925605

Unrolling Post-Mortem 3D Fingerprints Using Mosaicking Pressure Simulation Technique

KAREN PANETTA[1], (Fellow, IEEE), SRIJITH RAJEEV[1], (Member, IEEE), K. M. SHREYAS KAMATH[1], (Member, IEEE), AND SOS S. AGAIAN[2], (Fellow, IEEE)

[1]Department of Electrical and Computer Engineering, Tufts University, Medford, MA 02155, USA
[2]Department of Computer Science, City University of New York, New York, NY 10016, USA

Corresponding author: Srijith Rajeev (srijith.rajeev@tufts.edu)

This work was supported in part by the National Institute of Justice FY 2014 Research and Development in Forensic Science for Criminal Justice Purposes (Evaluation of the Use of A Non-Contact, 3D Scanner for Collecting Postmortem Fingerprints) under Grant 2014-IJ-CX-K003.

ABSTRACT Post-mortem fingerprints are a valuable biometric used to aid in the identification of a deceased individual. However, fingerprints from the deceased undergo decomposition leading to indefinite structure when compared to ante-mortem fingerprints. Moreover, the performance of the existing two-dimensional (2D) fingerprint recognition systems is still below the expected potential. These problems arise because fingerprints are generally captured by manipulating a finger against a plane. In post-mortem fingerprint recovery, the decedent's finger must go through several reconditioning processes to prevent the rapid onslaught of decomposition. To address these deficiencies associated with the 2D systems, three-dimensional (3D) scanning systems have been employed to capture fingerprints. The 3D technology is still in its transient phase and is limited primarily by 1) the lack of existing 3D databases; 2) the deficiency of 3D-to-2D fingerprint image mapping algorithms, 3) the incapacity to model and recreate the 2D fingerprint capturing procedure to improve 3D-2D fingerprint verification; and 4) the inability to apply traditional fingerprint unrolling techniques on post-mortem 3D fingerprints. This paper presents a novel method to perform post-mortem 3D fingerprint unrolling and pressure simulation to produce fingerprint images that are compatible with 2D fingerprint recognition systems. The thrust of this paper strives to: 1) develop a correspondence between 3D touchless and contact-based 2D fingerprint images; 2) model fingerprints with deformities to provide a viable fingerprint image for matching and; 3) develop a mosaic pressure simulation (MPS) algorithm to recreate the effects of 2D fingerprint capturing procedure.

INDEX TERMS 2D processing, 3D processing, ante-mortem, authentication, biometric, fingerprint, forensics, image-stitching, modeling, post-mortem, pressure-simulation, processing, recognition, unraveling, unrolling, verification.

I. INTRODUCTION

Biometrics refers to any human physiological or behavioral trait, which can be used for identification and verification [1], [2]. The need for biometrics can be found in federal, state, and local governments, military and commercial applications. There are several biometric modalities such as fingerprint, palm print, footprint, face, iris, retina, voice, keystroke, ear, and hand geometry [3], [4]. Among them, fingerprints have the most prevalent form of easily retrievable evidence as they provide better security, higher efficiency (low error rate), user convenience and feasibility (low-cost processing, expense) [5]. Numerous approaches for fingerprint verification exist, such as minutiae matching [6]–[8], basic pattern matching, and moiré fringe patterns [9], [10].

Fingerprint capturing technology has advanced from ink-based to sensor based, to three-dimensional (3D) fingerprint acquisition technology [8]. Ink-based acquisition is obtained by applying ink on the finger surface, pressing the finger face first onto a card, or rolling the finger from one side of the nail to the other on a card, and then finally, scanning the card to generate a two-dimensional (2D) digital

The associate editor coordinating the review of this manuscript and approving it for publication was Adam Czajka.

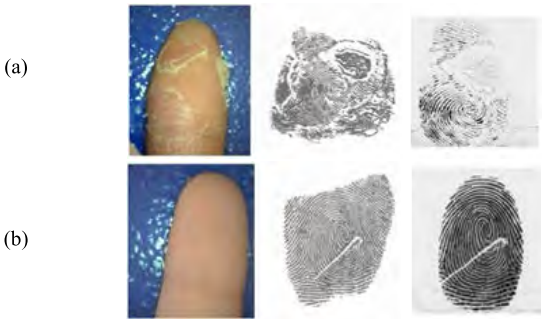

FIGURE 1. Fingerprints affected by skin-diseases. (a) Images show the distortions in fingerprints due to Psoriasis and (b) images show the distortions in fingerprints due to cuts (images recreated from [19]). *Note: Fingerprint impressions would be reversed during acquisition.*

image [11]. In sensor based acquisition, rolled or slap fingerprints are obtained by rolling/ pressing a finger over a sensor [12], [13]. A sensor-based system is one of the most prevalent commercially used systems, and it has a plethora of tools for processing and recognizing 2D fingerprint images. However, the performance of the state-of-the-art fingerprint recognition systems is below the expected potential. This is because of complications, such as (i) non-linear plastic distortions, which arise due to non-uniform pressure applied by an individual onto the scanner, (ii) variability in minutiae markup by forensic examiners, (iii) accumulation of dirt, (iv) improper finger placement, and (v) sensor noise. These techniques require a trained fingerprint acquisition expert to assist the user in pressing/rolling the finger on the sensor [14]–[16]. Moreover, the accuracy of 2D fingerprinting recognition systems is profoundly reliant on the quality of the image [17], [18].

An often-neglected facet in 2D fingerprinting is the condition of the finger itself. Skin diseases such as Eczema (rash - curable), Verruca Vulgaris (wart), and Psoriasis (scaly rash - incurable) [19], and cuts/bruises change the fingerprint features temporarily or permanently. This can be visualized in Figure 1.

Forensic-biometric identification, particularly post-mortem fingerprints of the deceased is crucial for criminal investigations. Post-mortem fingerprints are the prints acquired from the deceased after the incident, whereas ante-mortem prints are the known prints stored in a database. However, matching post-mortem and ante-mortem fingerprints is quite tedious and cumbersome [20]. It is also one of the most complex problems in the identification of unidentified human remains during singular deaths or mass disasters. Post-mortem fingerprint recovery is considered as a scientific identification modality, and it necessitates that all post-mortem technicians possess adequate training with a scientific background. This training is extensive, expensive, and requires large resources. Immaculate documentation and photography of the decedent's fingers must be performed before the procedure. The decedents' fingers must also go through reconditioning processes to prevent the rapid onslaught of decomposition [21]–[25]. Traditional techniques such as ink and stock fingerprint card, adhesive lifter, and livescan are employed to acquire fingerprints with deformations. The sample is recorded by physically manipulating the recording medium against the post-mortem finger [26], [27]. Moreover, post-mortem fingerprints do not have a definite structure and are altered due to decomposition. Also, unlike traditional fingerprints, post-mortem fingerprints may be missing features and have deformities, which can lead to a higher error rate. State-of-the-art 2D fingerprint systems are not capable of modeling the deformities to provide viable fingerprint images.

Contactless or touchless biometric identification systems use sensors, such as ultrasound sensors [28] and single cameras to capture fingerprint images. Although these systems have overcome a few of the problems of touch-based systems, they present other complications in fingerprint imaging. Ultrasound sensors are not widely used due to their substantial cost and size, and single cameras have a low field-of-view [29]. To overcome these problems, multi-view touchless sensing techniques are implemented [30], [31]. However, these systems pose the same problems as 2D fingerprint images; that is, scarred or post-mortem fingerprints may be deformed, and these systems are not capable of modeling them to provide viable images for matching.

A growing realization in the field of forensics and biometrics is that a human finger cannot be represented by a 2D form without loss. However, most establishments concentrate on recognizing individuals using 2D techniques. It led to the advent of 3D scanners as they provided a different scope for biometric verification [32]–[35]. They add depth, volume, and texture among other 3D properties, to the list of biometric characteristics that can be measured, thus making them more robust and versatile [36], [37].

Chen [11] developed a system that generated a 3D image of a finger using a projector and camera (based on Structured Light) [38]. Similarly, 3D reconstruction can be performed using stereo, or a sequence of images or videos [39], [40]. 3D fingerprint scanners have unlocked various possibilities to strengthen biometric security [41]. However, 3D technology poses problems such as (i) susceptibility to sensor noise, (ii) lack of modeling or mapping of post-mortem or deformed images in the state-of-the-art methods, and (iii) deficiency of affordable technology and resources that can make use of them [33].

Agencies around the world have an extensive collection of touch-based and touchless fingerprint databases [42], but the technology required to map from 2D to 3D is not feasible [43]. Current law enforcement agencies use different acquisition methods, which requires the interoperability of fingerprint templates. Additionally, agencies use fingerprint databases that are stored at the local, state, and federal level. A nationwide transition of 2D to 3D biometric authentication will incur a significant expense in terms of time and finance.

During acquisition, a curved human finger is flattened on a 2D plane, thus shifting the features in different orientations [44]. The quality of the fingerprint image is also dependent on individual artifacts such as skin conditions

FIGURE 2. An illustrative example of different pressure simulations on the same finger. Features will be displaced in different directions for different amounts of pressure.

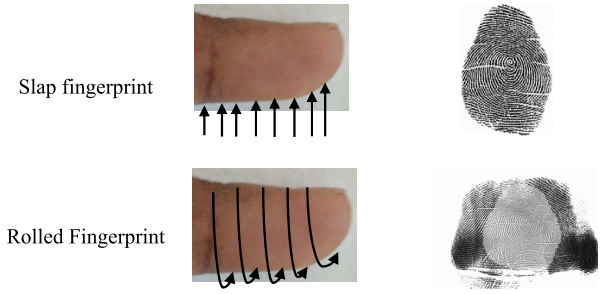

FIGURE 3. Shows the direction of pressure simulation and output for slap and rolled 2D fingerprint (left to right or right to left) acquisition techniques.

as well as deformations and pressure applied [45]. Different individuals may exert different levels of pressure which results in different variations of fingerprint [46]. This phenomenon is illustrated in Figure 2 and Figure 3. However, in a 3D system, due to its touchless properties, these variations in ridges and valleys are not present. Therefore, matching 2D and unrolled 3D fingerprints may lead to erroneous results [34]. Hence, there is an imminent need for a realistic 3D to 2D fingerprint mapping system to facilitate post-mortem biometric verification.

Some of the problems mentioned previously can be solved by using 3D capture modeling. The process involves (i) capturing a 3D image of the deceased's finger after reconditioning and recovering, (ii) modeling the object onto a flat surface whilst maintaining the ridge mesh integrity and considering the severe deformations that may exist on the post mortem finger, (iii) resampling the unrolled image to improve structural integrity, (iv) rolling back the flat 3D image to the shape of a finger, (v) dividing the 3D image into 'n' cross-sections and then simulating pressure on each cross-section, and (vi) mosaicking each cross-section to provide an unrolled pressure simulated finger image. This process is repeated iteratively with different levels of pressure to improve the probability of finding a correct match. Ante-mortem fingerprints can also be unrolled using pressure simulation technique by performing steps (i), (v), and (vi). The afore-mentioned initial unrolling process is an extension of Rajeev's (2014) non-parametric unrolling approach [51].

Fingerprint mosaicking is a technique widely used in multi-view touchless fingerprint systems to combine images captured from different cameras. It involves the combination of information obtained from multiple images to generate a single complete or panoramic image. Some of the main challenges in mosaicking are: finding or generating the best seam line, visibility of the seam line after mosaicking, and color variations in the combined images [52], [53]. To tackle all these problems, Rao *et al.* [54] developed a new correlation technique called the alpha-trimmed correlation algorithm to mosaic finger images. The proposed Mosaic Pressure Simulation (MPS) algorithm utilizes the concepts of image mosaicking to stitch multi-views of the pressure simulated 3D finger.

This paper describes (i) an extended unrolling framework that can efficiently unroll post-mortem fingerprints and (ii) a Mosaic Pressure Simulation (MPS) algorithm that can recreate the effects of 2D fingerprint capturing procedure. The presented system can unroll and simulate rolling pressure on a 3D deformed post-mortem or ante-mortem finger images. The rest of this paper is organized as follows: in Section II, descriptions of related systems are presented. In Section III, the extended unrolling framework is described. Section IV describes the MPS system. Performance analysis and comparisons are given in Section V. Finally, conclusions are drawn in Section VI.

II. RELATED WORK

This section discusses the existing systems and methods in unrolling 3D images. The 3D modeling process called unrolling refers to the representation of a 3D image's surface as a 2D image. In other words, it is the procedure of unfolding a 3D image onto a 2D plane. In this process, the letters "U" and "V" are used to denote the axes of the 2D image as "X," "Y" and "Z" denote the axes of the object in 3D space [55], [56]. This process has a wide variety of applications in fields such as gaming industry, medical imaging, industrial designs, surface recognition, and map projection [57]. Representation of the data would be preferable on a 2D plane to work with these applications [33].

Focusing on the conversion of a 3D fingerprint to a 2D flat image, pre-processing may be necessary to improve the quality of the image as explained in [58]. Several unrolling algorithms have been proposed which can unwrap 3D images. Unrolling [49] or unraveling [43] algorithms can be divided into two classes, namely parametric (best fit) and non-parametric [33], [49].

A. PARAMETRIC UNROLLING TECHNIQUE

In this approach, the 3D finger is closely approximated to the shape of a known 3D entity such as a sphere, ring, or cylinder. A few parametric techniques are mentioned in Table 1. The unrolled outputs may have a sizeable stretching effect if the shapes are not identical. The main drawback of parametric approaches is that they assume the shape of a human finger to be a known and fixed entity. This is because, a human finger may be bulky or thin, may be uneven or smooth, differing from individual to individual. These variations increase infinitely when deformed 3D fingerprints are considered.

TABLE 1. Parametric unrolling approaches.

Author	Description
Chen, (2006) [33]	Unrolls the 3D finger by approximating it to a cylindrical surface. This approach assumes that the human finger is a collection of circles of equal radius stacked one above the other. Thus, every point of the finger is projected onto a cylinder.
Wang, (2010) [48]	3D finger images are unrolled using a fit sphere approach. The distance between the sphere and the finger is then calculated.
Abramovich, (2010) [49]	Unravels the finger using circular estimates of cross-sections of the 3D finger image. This approach is useful for normal slap fingerprint verification.
Wang, (2010) [34]	Presented another approach that assumed that the human finger is a collection of circles of different radii. These radii are approximated to fit into the peaks and valleys of the human finger.

TABLE 2. Non-parametric unrolling approaches.

Author	Description
Chen, (2006) [33]	This approach first upsamples the finger image to increase the density. Then each cross-section of the finger is unrolled. Theoretically, though this approach produces better results, it does not take into account, the variations caused by unrolling the fingerprint ridges and valleys as well.
Zhao, (2011) [50]	A post-processing method to simulate slap level pressure on the unrolled finger image was presented.
Fatehpuria, (2006) [43]	This approach extracts the surface of the 3D finger image using a weighted, non-linear, least square algorithm before unrolling. The extracted surface is then unrolled using springs algorithm
Shafaei, (2009) [51]	Unrolls the 3D finger similarly to Fatehpuria, (2006) [43], and then uses curvature analysis to superimpose the fingerprint texture on the unrolled surface.
Rajeev, (2016) [52]	This technique unrolls post-mortem fingerprints into equivalent 2D fingerprints. However, it did not concentrate on the effects of pressure.

B. NON-PARAMETRIC UNROLLING TECHNIQUE

Non-parametric unrolling algorithms utilize the angular relation and Euclidean distance between two successive points in the 3D mesh [33], [59]. These algorithms compute the corresponding pixels in the 2D equivalent fingerprint image from the points in the 3D finger image. Some of the implementations of this approach are shown in Table 2. Most of the literature assumes a non-deformed/regular 3D finger image, i.e., they are not designed for 3D images with deformities or images affected by pressure.

After an extensive literature search, the authors have concluded that the state-of-the-art unrolling methods do not accurately simulate the rolling pressure exhibited during the physical rolling fingerprint acquisition [60].

III. EXTENDED UNROLLING FRAMEWORK

This section presents an improvement and extension of Rajeev's [51] non-parametric unrolling approach. Both algorithms can unroll a 3D finger (normal or deformed) image into a flat and uniform 3D finger mesh. However, the extended algorithm can resample the mesh to improve mesh density, and it can be applied to both ordered and non-ordered point-clouds. This process is developed to make it compatible for verification of a 3D finger with a 2D fingerprint database. Figure 4 shows the work-flow involved in the extended unrolling algorithm. A comprehensive explanation of the unrolling algorithm is explained in the subsequent segments:

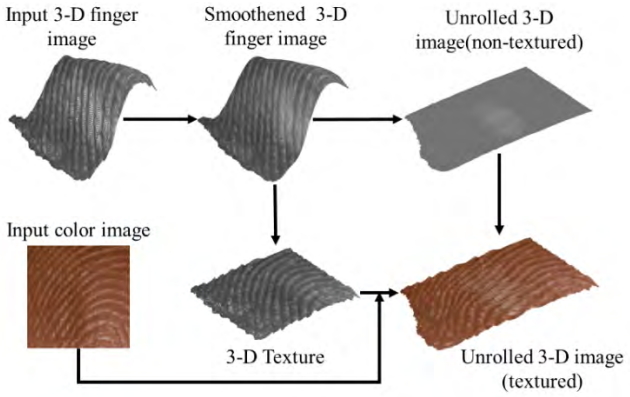

FIGURE 4. Shows the work-flow involved in unrolling the deformed 3D finger. [Row 1] The input finger is de-texturized using a smoothing filter, followed by unrolling. [Row 2] Finally, the color and texture are mapped back to the unrolled 3D image. Note: A zoomed cross-section is shown for visual purposes.

A. ANOMALY REMOVAL AND TEXTURE EXTRACTION

A raw fingerprint image may have unnecessary background noise and undefined boundaries. A Gaussian filter (1) is used to filter the noise and smoothen the 3-D texture. The smoothed 3D image is used for unrolling purposes, and the difference between the original (3D) image and the Gaussian filter output (3D) provides the texture ($P(x, y, z)^{i,j}_{extracted}$) of the finger.

$$g(i,j) = \frac{1}{2\pi\sigma^2} \cdot exp\left(-\frac{i^2+j^2}{2\sigma^2}\right) \quad (1)$$

where σ^2 is the variance of the Gaussian filter, i and j are the distance from the origin along the horizontal axis and vertical axis respectively. The depth co-ordinates are convolved with this filter.

B. 3D FINGER IMAGE UNROLLING

Unrolling is necessary to provide interoperability between 3D and 2D systems. Parametricp unrolling methods depend on the knowledge of the shape of the system and are henceforth less robust. Therefore, an unrolling algorithm is presented that considers the existence of deformities and finds countermeasures to unroll the 3D finger images effectively. The following two sections describe two 3D finger unrolling methods, i.e., without and with anomalies.

1) 3D IMAGES WITHOUT ANOMALIES

Few 3D reconstruction algorithms fill holes in the 3D image during mesh surface reconstruction. In such circumstances, non-parametric unrolling is performed by directly calculating the Euclidean distance between corresponding points. Equations (2-3) perform the regular non-parametric unrolling operation.

$$D_y(i,j) = \sqrt{(x(i,j) - x(i,j+1))^2 + (z(i,j) - z(i,j+1))^2} \tag{2}$$

$$\bar{x}(i,j+1) = \bar{x}(i,j) \pm D(i,j) \tag{3}$$

where x, y, and z are the surface, height, and depth coordinates, D be the Euclidean distance, and $\bar{x}$ is the new surface co-ordinates. The algorithm can be performed along the surface or the height, i.e., x and y are inter-changeable.

2) 3D IMAGES WITH ANOMALIES

Few biometric 3D scanners may avoid filling holes while performing surface reconstruction because they generate artificial data. Therefore, this paper makes use of a compensation model developed by Rajeev, [51] to perform non-parametric unrolling. The compensation model can be obtained by determining and saving the location of the last valid point in the row according to (4-5). These estimates are used in (6-7) to unroll the 3D image.

$$\begin{aligned} &if\ (f(i,j) == 0\ \&\&\ f(i,j-1)! = 0) \\ &\quad \hat{f}(i,j) = f(i,j-1) \end{aligned} \tag{4}$$

$$\begin{aligned} &if\ f(i,j) == 0\ \&\&\ f(i,j-1) == 0 \\ &\quad \hat{f}(i,j) = \hat{f}(i,j-1) \end{aligned} \tag{5}$$

$$D_y(i,j) = \sqrt{(\hat{x}(i,j) - x(i,j+1))^2 + (\hat{z}(i,j) - z(i,j+1))^2} \tag{6}$$

$$\bar{x}(i,j+1) = \dot{x}(i,j) \pm D(i,j) \tag{7}$$

where $f = P(x,y,z)$ and $\hat{f} = P(\hat{x}, \hat{y}, \hat{z})$, P is a 3D point, x, y, and z are the surface, height, and depth respectively, $\dot{x}$ possesses the last known real unrolled surface output in the current row. $\hat{x}$, $\hat{y}$, and $\hat{z}$ are the 3D co-ordinates of the points in the compensation model. The depth information is discarded after running the unrolling algorithm.

C. TEXTURE FUSION

To create a realistic 3D finger image, the original color and texture should be incorporated into the unrolled output. The unrolled 3D image is a smooth and flat equivalent 2D image. The texture saved while pre-processing is applied to provide additional features for fingerprint recognition systems. This step is vital to include the ridges and valleys of the original 3D finger image into the unrolled finger image.

If the input point-cloud is an unorganized (or unordered) point-cloud, it is first converted to an organized (ordered) point-cloud. An organized point cloud is ordered as a 2D array of points, while an unorganized point-cloud is a one-dimensional array. In this paper, texture fusion involves a direct one to one mapping using equation (8) [61].

$$\begin{aligned} &For\ every\ i,j = 1\ to\ dimensions\ of\ pointcloud \\ &P(x,y,z)^{i,j}_{textured} = P(x,y,z)^{i,j}_{unrolled} + P(x,y,z)^{i,j}_{extracted} \end{aligned} \tag{8}$$

D. 3D UNROLLED FINGER IMAGE RESAMPLING

Resampling a deformed 3D image may increase the noise in the image, and thus the unrolling process may get hindered. On the other hand, resampling after unrolling will increase the quality of the model and thus, help in verification. The process of resampling is similar to image interpolation, but 3D resampling occurs across the surface, height and, depth. The X, Y, and Z coordinates are upsampled by placing zeros between consecutive points. If there exists no point adjacent to a point before up-sampling, then it is presumed that no points exist in that region. Thus, that region is excluded from interpolation after upsampling. In all other cases, interpolation is performed using a window of size (1x3). Linear interpolation is performed as shown in (9).

$$P(X,Y,Z) = \left(P(X,Y,Z)^- + P(X,Y,Z)^+\right)/2 \tag{9}$$

where $P(X,Y,Z)$ represents the current point co-ordinates, + and – represent the next and the previous co-ordinates respectively.

IV. MOSAIC PRESSURE SIMULATION (MPS)

This process is performed to replicate the distortions that occur during the acquisition of a 2D fingerprint. The following algorithm describes the general method of simulating pressure on the 3D finger image:

The following sections explain the Mosaic Pressure Simulation (MPS) algorithm:

A. NO-REFERENCE DEPTH CALCULATION

This stage can be skipped if the original 3D finger image is not deformed. The amount or lack of deformity can be determined by measuring the standard deviation of the 3-D finger within the finger boundaries. Otherwise, the unrolled

Algorithm 1 Pressure Simulation

1. Map the unrolled fingerprint to shape of a finger.
2. Provide the number of faces
3. Determine the geometry of 3D fingerprint
4. Determine the location of the face endpoints.
5. Calculate the surface length and depth of each region.
6. Calculate the chord length from the data obtained.
7. Calculate the pressure simulated depth

flat finger image is mapped to the shape of a finger by determining the geometry of the unrolled 3D image. The distance between the first and last point for a given slice provides the approximate diameter of the 3D finger. The depth is calculated using (10-14). Let X and Z be the surface and new depth co-ordinates, D and h be the approximate width and height of the finger. Parameter t describes the ratio of depth at the top of the finger to the bottom of the finger.

$$\Delta X = |X(i, j) - X(i, 1)| \tag{10}$$

$$D_1 = D - D * t \tag{11}$$

$$b = (D - D_1) / log(h) \tag{12}$$

$$D_{11} = D_1 + b * log(h_i) \tag{13}$$

$$Z(i, j) = \sqrt{D_{11}^2/2 - \Delta X^2} \tag{14}$$

B. PRESSURE SIMULATION ON CROSS-SECTIONS OF FINGER

Once a non-deformed 3D finger image is obtained, the rolling pressure can be simulated. This process requires the knowledge of the geometrical parameters of the 3D image, such as (i) the width of the finger, i.e. the distance between the first and last point of the model (approximated, in case of post-mortem fingerprint), (ii) the number of segments, (iii) total number of points that exist along that segment, (iv) the surface length (i.e., from one end to the other end) and the maximum depth of each segment is determined, and (v) the length of the chord for each segment is calculated, which will act as a reference scale. Figure 5 provides an illustrative example of the direction of the pressure applied to the finger.

Application of pressure is mimicked by changing the depth of the points in the selected face with the reference scale. A point in the face, which has the maximum depth is chosen as the starting point. The new pressure simulated depth coordinates are calculated using the distance between successive surface points and the reference scale as shown in (15).

$$\tilde{Z}(i, j) = Z\left(\bar{\bar{i}}, a(k)\right) + \sqrt{(c(k) - count * \bar{c}(k))^2 - (s(k) - count * \bar{s}(k))^2} \tag{15}$$

where count is the location of the current point with respect to the segment, c and s are the chord and surface information respectively. This process is repeated for all the segments. Finally, a 2D image of each segment including partial neighboring faces is captured for final image stitching.

FIGURE 5. Shows the pressure simulation lines. Pressure will be simulated along the normal of each line. Increasing the number of slices will produce a genuine rolling effect but, increases computational cost.

C. MOSAICKING OR IMAGE STITCHING

The final stage of the algorithm includes a mosaicking process which combines all the pressure simulated faces to obtain one unrolled image. It can be achieved by blending the input images into a single mosaic, or by integrating the feature sets of the input images. The alpha-trimmed correlation approach developed by Rao *et al.* [54] is used to perform multi-finger image mosaicking. Since major portions of these images will have the same texture, Scale-Invariant Feature Transform (SIFT) (20) can be used for feature extraction to obtain correspondences between these images. Matching is performed by comparing these feature points.

Generally, errors in the overlapping images lead to geometric misalignments and photometric differences. The most critical and final stage in producing a perfectly mosaicked image is image blending. This process will mosaic the pressure-simulated 3D image together, obtaining an unrolled 2D fingerprint, which will mimic the pressure distortions produced on a 2D fingerprint while using a 2D scanner. These two sets are mosaicked together to get one final unrolled image.

V. COMPUTER SIMULATIONS

A. 3D FINGER MODEL INITIALIZATION

There are no pre-existing post-mortem datasets. FlashScan3D [62] provided a post-mortem database, and it was constructed by simulating deformities on a few ante-mortem prints. The database included a total of thirty ante-mortem 3D images and three severely deformed 3D post-mortem finger images. The mean and standard deviation of the depth images are shown in Figure 6. The finger images are in the MAT5 format [62], [63]. Figure 7 (a) shows a sub-section of the 3D finger images used in the presented work. Furthermore, the authors did not have access to the actual pressed or rolled fingerprint impressions. Additionally, this database did not have any id tags or numbers that could be used for recognition purposes.

B. UNROLLING

The 3D images are filtered to remove anomalies (result shown in Figure 7 (b)). Then, the filtered 3D images are smoothened, and the color and texture are captured. Next, the smoothened image is unrolled to a plane surface and the texture and color are fused. All the images in the database were successfully unrolled and resampled into an equivalent 2D fingerprint based on the unrolling algorithm described in section III.

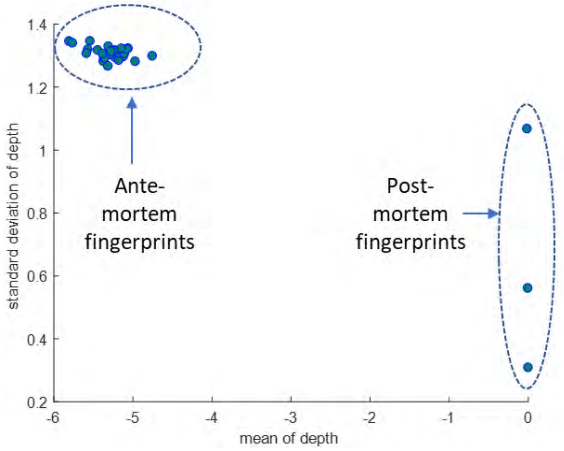

FIGURE 6. Shows the depth distribution of the 3D fingerprints in terms of mean and standard deviation. The 30 ante-mortem fingerprints have similar depth properties, while the post-mortem prints have highly varying properties.

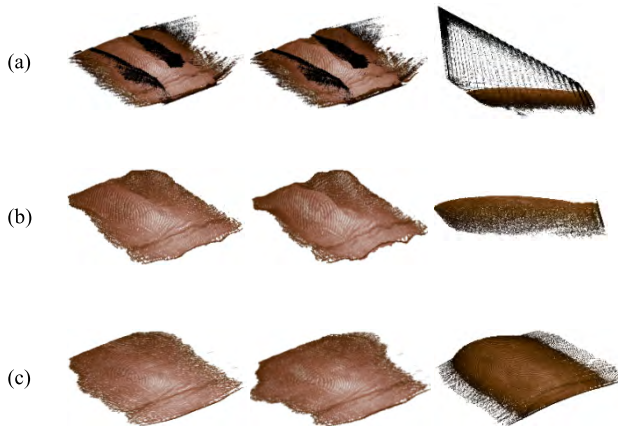

FIGURE 7. Examples of biometric 3-D unrolling. (a) shows the 3D input image captured using FLASHSCAN3D [62] (with reconstruction noise), (b) shows the 3D images after noise (anomaly) removal, and (c) shows the unrolled 3D images (output).

The output of the unrolling phase is shown in Figure 7 (c). Visual inspection of the unrolled images demonstrates the success of the algorithm.

C. PRESSURE SIMULATION

For number of faces (N=4), four sections of the 3D image (Figure 8(a)) were individually pressed and named as images 1,2,3, and 4 and collectively called as SET A (shown in Figure 8(b)). Furthermore, three more images were created, which have a shared pressed region with at least two images from SET A. They were named as 5, 6, and 7 and are part of SET B (shown in Figure 8(b)). Figure 8(c) shows the cross-sections of the pressure simulated images which will be stitched together. A similar process was performed for N=5 and 6.

D. MOSAICKING

Figure 9 shows the order that the algorithm used for mosaicking multi-finger 3D images. For instance, images 1 and 5 are stitched to obtain image 1-5 and so on. The final image '1-5-2-6-3-7-4' is an unrolled fingerprint image which will have incorporated all the pressure simulations evenly.

The mosaicking algorithm determines the region of interest between the images and then obtains the best-fit seam line through alpha-trimmed correlation (shown in Figure 10 (a)). Finally, the images are mosaicked together to obtain a single image.

Figure 11 shows some of the results of unrolling and pressure simulation. As the number of faces is increased, the amount of pressure applied increases, as well as the complexity of the algorithm. This process of applying pressure and mosaicking can be repeated for different pressure parameters. The number of faces that can be pressed can also be changed depending on the user's requisites. With the exception of cases in which there is considerable injury or deformity of the fingerprint, the results of the MPS can be used for automated/manual biometric verification/authentication. MPS can be applied to both ordered and unordered point-clouds [64].

TABLE 3. No reference quality measure definitions.

$AME_{k1,k2} = -\frac{1}{k_1 k_2}\sum_{k=1}^{k_1}\sum_{l=1}^{k_2} 20\ln\left(\frac{I_{max;k,l} - I_{min;k,l}}{I_{max;k,l} + I_{min;k,l}}\right)$
$SDME_{k1,k2} = -\frac{1}{k_1 k_2}\sum_{k=1}^{k_1}\sum_{l=1}^{k_2} 20\ln\left(\frac{I_{max;k,l} - 2\,I_{center;k,l} + I_{min;k,l}}{I_{max;k,l} + 2\,I_{center;k,l} + I_{min;k,l}}\right)$
$EME_{k1,k2} = \frac{1}{k_1 k_2}\sum_{k=1}^{k_1}\sum_{l=1}^{k_2} 20\ln\frac{I_{max;k,l}}{I_{min;k,l}}$
NR color measure= $c1$ * *colorfu* lness + $c2$ * *sharpness* + $c3$* *contrast*

E. EVALUATION

Numerous factors affect the performance of a fingerprint recognition system; however, image quality of the fingerprint features is the most important part that can affect overall performance of a biometric system. The MPS output images are subjected to a wide variety of distortions and changes during capture, pre-processing, unrolling, pressure simulation, and image mosaicking. Research has shown that such operations deter the visual and structural quality of the images [65]. Thus, this sub-section evaluates the visual and structural quality of the images using no-reference (NR) based measures. Image enhancement measures based on Weber's and Michelson contrast law- Measure Of Enhancement or Measure Of Improvement [66], (EME) [67], Michelson Law EME (AME) [68], SDME [69], [70], and No-reference color measures [71] have been previously proposed. The definitions of these measures are listed in Table 3. The definitions for colorfulness, sharpness, and contrast can be found in [71]. The magnitude of the score describes the quality of the image. NFIQ is the first publicly available fingerprint quality assessment tool (provided by NIST) [72]. NFIQ is used to link image quality

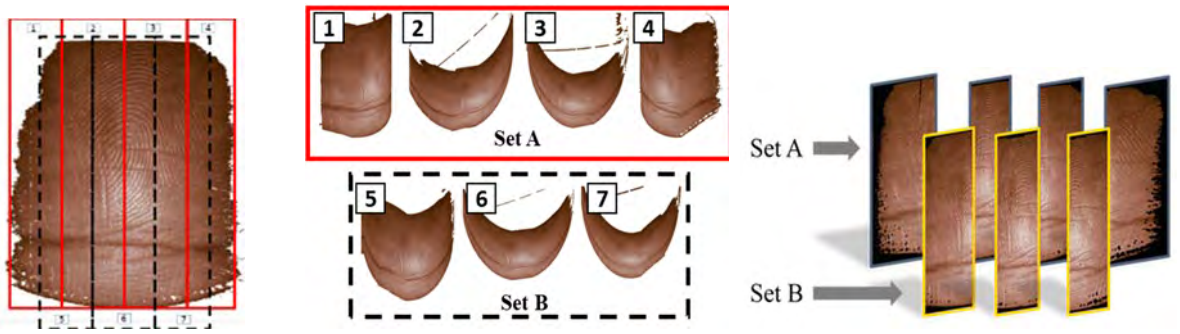

FIGURE 8. Pressure simulation and slice extraction. (a) shows the areas where the pressure will be simulated. Areas in red will form Set A, and areas in dotted black will form Set B, (b) shows the pressure simulated of set A and set B, and (c) shows the pressure simulated segments of set A and set B. These images are mosaicked together using the alpha-trimmed correlation method. Note: This order is one of the many combinations that can be used. These smaller sets have been chosen for visual and explanation purposes.

TABLE 4. No reference quality measure results for the MPS images.

Measure	Unrolled	Pressure simulated N=4	Pressure simulated N=5	Pressure simulated N=6
AME (mean)	16.6687	21.9314	23.2027	22.7161
SDME (mean)	29.3698	35.6478	36.9401	36.4427
EME (mean)	4.6339	2.4368	2.2015	2.2065
NR color measure (mean)	1.0176	0.6376	0.5962	0.6252
NFIQ (mean) [74]	3	2.75	3.25	3.25
Note: Total number of images used =33				

TABLE 5. Average number of minutiae detected (for minutiae quality > 0.1).

Total images=33	Unrolled	*Pressure simulated N=4*	*Pressure simulated N=5*	Pressure simulated N=6
Average number of minutiae (MINDTCT) [74]	35	53	41	49

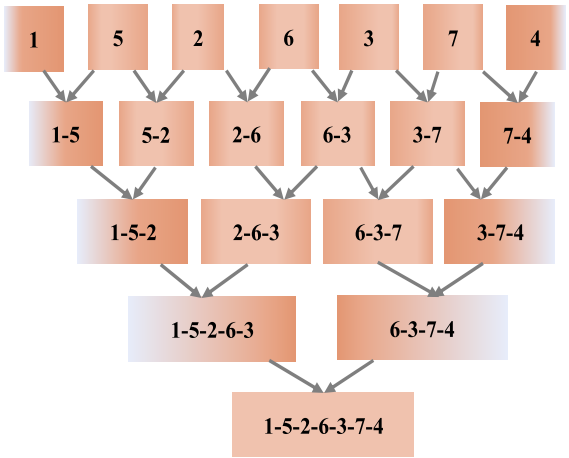

FIGURE 9. Shows one of the combinational methods involved in mosaicking the pressure simulated images. These images are mosaicked together using the alpha-trimmed correlation method [54].

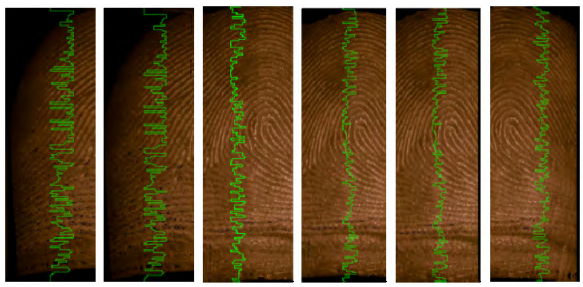

FIGURE 10. Different stages of the mosaicking algorithm for two sample images, (a) shows the region of interest and seam lines for different pressure images.

to operational recognition performance [72]. A lower NFIQ score indicates higher quality. The MPS output images were subjected to the afore-mentioned standard image error measurement techniques, and the results are tabulated in Table 4. Based on the scores, it can be inferred that the MPS output images are generally better than the original 2-D equivalent fingerprint (unrolled) in terms of quality.

Furthermore, the average number of miniutiae in the fingerprint images were calculated using the ''mindtct'' application [74] from the NIST Biometric Image Software (NBIS). The results are shown in Table 5. For pressure simulation parameter N=4, 5, and 6, the average number of minutiae increased by 51.42 %, 17.14%, and 40.00% respectively.

Although there are a few existing fingerprint unrolling algorithms, comparing them with the proposed technique seems unfair as the state-of-the-art techniques were not designed for post-mortem 3D unrolling. For instance, the algorithm developed by Chen *et al.* [33] requires a

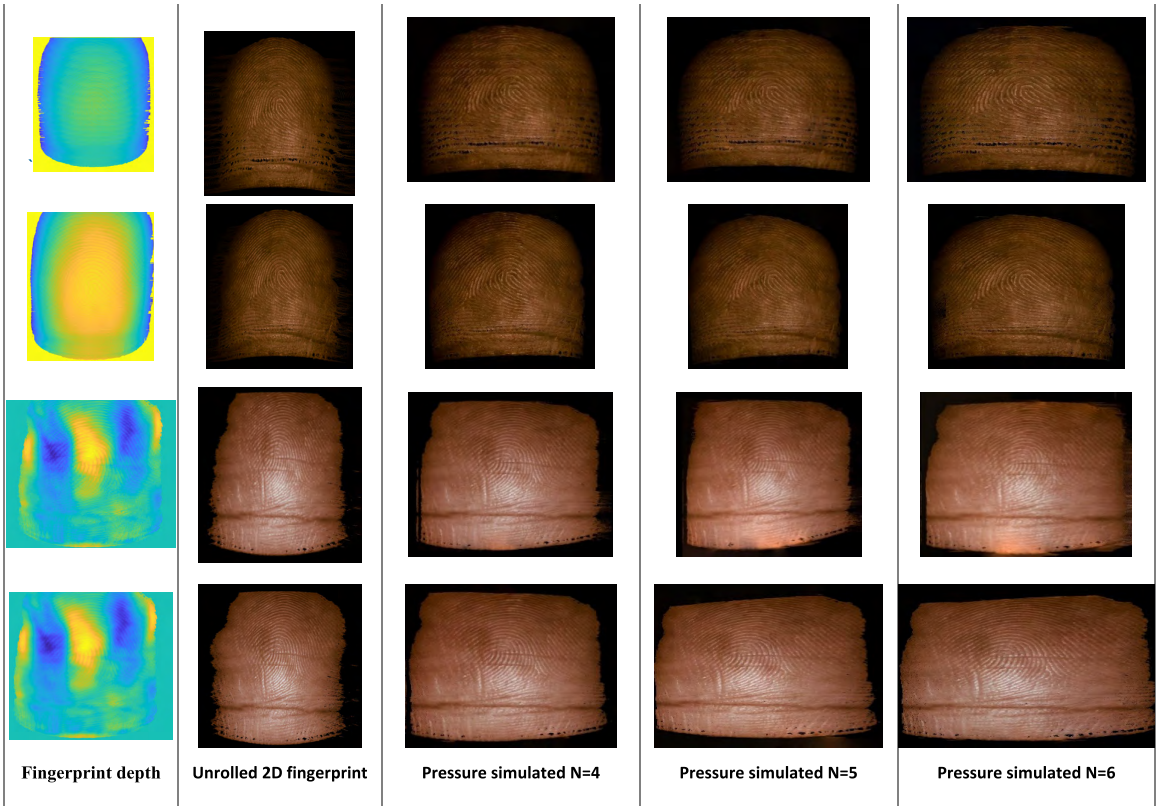

FIGURE 11. Shows the output image of the unrolling algorithm and pressure simulation with different parameters, where the first column shows the actual fingerprint depth, the second column shows the unrolled fingerprint image, and the remaining columns show the pressure simulated images with different values for the number of faces (N).

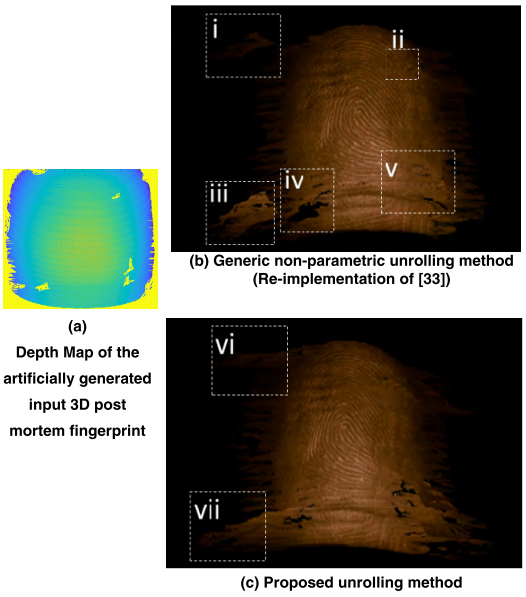

FIGURE 12. General comparison of unrolling algorithms; regions i and iii show disconnected pieces of the skin; regions ii and v show that the original holes have been covered by the unrolled skin; region iv shows that the holes have stretched; vi and vii show the stretching effect of the proposed unrolling method. ***Note: The input image was artificially created and was not used in the evaluation stage described earlier.***

dense representation of the fingerprint. However, when the algorithm (Re-implemented by the author) is applied to a post-mortem fingerprint with holes, it will fail as shown in figure 12. This is because a hole is usually represented by $X = 0$ in the world space. One of the limitations of the proposed method is the stretching effect that can be visualized in figure 12 (c).

A small dataset is not sufficient to draw conclusive results. However, there is no pre-existing post-mortem dataset, and there are additional hurdles to overcome in terms of consent and access when trying to obtain data from deceased individuals. A total of thirty (normal or ante-mortem 3D) + three images (deformed or post-mortem 3D) were processed using the proposed method.

VI. CONCLUSION

The viability of post-mortem fingerprints is limited due to decomposition. Therefore, a non-invasive method to acquire, process and solve pressure distortions is required. In this paper, an extended unrolling framework and a novel Mosaic Pressure Simulation (MPS) algorithm were proposed. MPS comprises innovative 3D pressure simulation and 2D mosaicking algorithms, combined with other processing techniques such as 3D filtering, 3D non- parametric unrolling, and 3D resampling. MPS solves the problem of interoperability of authenticating 3D and 2D fingerprint images effectively by producing realistic images. It particularly can be used to solve the problem of rolling pressure distortions in fingerprints. The robustness of the algorithm was tested by unrolling fingerprints with different depth

constraints. Computer simulations demonstrated that MPS could be a useful tool to unroll post-mortem fingerprints for identification purposes. Consequently, MPS can be used to achieve reliable ante-mortem/post-mortem recognition. MPS can be used as an intermediary step to find correspondences between 2D and 3D fingerprint until a time comes when 3D to 3D matching is entirely feasible.

ACKNOWLEDGMENT

The authors would like to thank FlashScan3D, LLC for providing 3-D and 2-D input database.

REFERENCES

[1] A. Jain, R. Bolle, and S. Pankanti, *Biometrics: Personal Identification in Networked Society*. New York, NY, USA: Springer, 2006.
[2] A. Toosi, A. Bottino, S. Cumani, P. Negri, and P. L. Sottile, "Feature fusion for fingerprint liveness detection: A comparative study," *IEEE Access*, vol. 5, pp. 23695–23709, 2017.
[3] S. K. K M, S. Rajeev, K. Panetta, and S. S. Agaian, "Comparative study of palm print authentication system using geometric features," *Proc. SPIE*, vol. 10221, May 2017, Art. no. 102210M.
[4] S. K. K M, S. Rajeev, K. Panetta, and S. S. Agaian, "Fingerprint authentication using geometric features," in *Proc. IEEE Int. Symp. Technol. Homeland Secur. (HST)*, Apr. 2017, pp. 1–7.
[5] A. K. Jain, A. Ross, and S. Prabhakar, "An introduction to biometric recognition," *IEEE Trans. Circuits Syst. Video Technol.*, vol. 14, no. 1, pp. 4–20, Jan. 2004.
[6] S. Liu and M. Silverman, "A practical guide to biometric security technology," *IT Prof.*, vol. 3, no. 1, pp. 27–32, Jan. 2001.
[7] E. H. Holder, L. O. Robinson, and J. H. Laub, "The fingerprint sourcebook," US Dept. Justice, Office Justice Programs, Nat. Inst. Justice, Washington, DC, USA, 2011.
[8] D. Maltoni, D. Maio, A. K. Jain, and S. Prabhakar, *Handbook of Fingerprint Recognition*. London, U.K.: Springer, 2009.
[9] A. Sankaran, M. Vatsa, and R. Singh, "Latent fingerprint matching: A survey," *IEEE Access*, vol. 2, pp. 982–1004, 2014.
[10] A. Sankaran, M. Vatsa, and R. Singh, "Multisensor optical and latent fingerprint database," *IEEE Access*, vol. 3, pp. 653–665, 2015.
[11] G. Parziale and Y. Chen, "Advanced technologies for touchless fingerprint recognition," in *Handbook of Remote Biometrics*. London, U.K.: Springer, 2009, pp. 83–109.
[12] V. I. Ivanov and J. S. Baras, "Authentication of swipe fingerprint scanners," *IEEE Trans. Inf. Forensics Security*, vol. 12, no. 9, pp. 2212–2226, Sep. 2017.
[13] J. Feng, S. Yoon, and A. K. Jain, "Latent fingerprint matching: Fusion of rolled and plain fingerprints," in *Advances in Biometrics*. Berlin, Germany: Springer, 2009, pp. 695–704.
[14] Z. Chen and C. H. Kuo, "A topology-based matching algorithm for fingerprint authentication," in *Proc. 25th Annu. IEEE Int. Carnahan Conf. Secur. Technol.*, Oct. 1991, pp. 84–87.
[15] D. Maltoni, "A tutorial on fingerprint recognition," in *Advanced Studies in Biometrics*. Berlin, Germany: Springer, 2005, pp. 43–68.
[16] R. D. Labati, A. Genovese, V. Piuri, and F. Scotti, "Toward unconstrained fingerprint recognition: A fully touchless 3-D system based on two views on the move," *IEEE Trans. Syst., Man, Cybern., Syst.*, vol. 46, no. 2, pp. 202–219, Feb. 2016.
[17] S. Bakhtiari, S. S. Agaian, and M. Jamshidi, "Local fingerprint image reconstruction based on Gabor filtering," *Proc. SPIE*, vol. 8406, May 2012, Art. no. 840602.
[18] Y. Chen, S. C. Dass, and A. K. Jain, "Fingerprint quality indices for predicting authentication performance," in *Audio- and Video-Based Biometric Person Authentication*, vol. 3546. Berlin, Germany: Springer, 2005, pp. 160–170.
[19] M. Dolezel, M. Drahansky, J. Urbanek, E. Brezinova, and T.-H. Kim, "Influence of skin diseases on fingerprint quality and recognition," in *New Trends and Developments in Biometrics*. Rijeka, Croatia: InTech, 2012.
[20] T. Kahana, A. Grande, D. Tancredi, J. Penalver, and J. Hiss, "Fingerprinting the deceased: Traditional and new techniques," *J. Forensic Sci.*, vol. 46, no. 4, pp. 908–912, 2001.
[21] D. Keating and J. Miller, "A technique for developing and photographing ridge impressions on decomposed water-soaked fingers," *J. Forensic Sci.*, vol. 38, no. 1, pp. 197–202, 1993.
[22] A. K. Datta, H. C. Lee, R. Ramotowski, and R. E. Gaensslen, *Advances in Fingerprint Technology*. Boca Raton, FL, USA: CRC Press, 2001.
[23] L. Richardson and H. Kade, "Readable fingerprints from mummified or putrefied specimens," *J. Forensic Sci.*, vol. 17, no. 2, pp. 325–328, 1972.
[24] F. Zugibe and J. Costello, "A new method for softening mummified fingers," *J. Forensic Sci.*, vol. 31, no. 2, pp. 726–731, 1986.
[25] W. Haglund, "A technique to enhance fingerprinting of mummified fingers," *J. Forensic Sci.*, vol. 33, no. 5, pp. 1244–1248, 1988.
[26] D. Porta, M. Maldarella, M. Grandi, and C. Cattaneo, "A new method of reproduction of fingerprints from corpses in a bad state of preservation using latex," *J. Forensic Sci.*, vol. 52, no. 6, pp. 1319–1321, 2007.
[27] M. Mulawka and L. S. Miller, *Postmortem Fingerprinting and Unidentified Human Remains*. Abingdon, U.K.: Routledge, 2014.
[28] W. Bicz, D. Banasiak, P. Bruciak, Z. Gumienny, S. Gumuliński, D. Kosz, and G. Rabiej, "Fingerprint structure imaging based on an ultrasound camera," *Instrum. Sci. Technol.*, vol. 27, no. 4, pp. 295–303, 1999.
[29] S. S. Agaian, M. Mulawka, R. Rajendran, S. P. Rao, S. K. K M, and S. Rajeev, "A comparative study of image feature detection and matching algorithms for touchless fingerprint systems," *Electron. Imag.*, vol. 2016, no. 15, pp. 1–9, 2016.
[30] H. Choi, K. Choi, and J. Kim, "Mosaicing touchless and mirror-reflected fingerprint images," *IEEE Trans. Inf. Forensics Security*, vol. 5, no. 1, pp. 52–61, Mar. 2010.
[31] A. Kumar, C. Kwong, and L. Yang, "Contactless 3D fingerprint reconstruction using photometric stereo," Hong Kong Polytech. Univ., Hong Kong, China, Tech. Rep. COMP-K-07, 2012.
[32] A. Kumar and C. Kwong, "Towards contactless, low-cost and accurate 3D fingerprint identification," *IEEE Trans. Pattern Anal. Mach. Intell.*, vol. 37, no. 3, pp. 681–696, Mar. 2015.
[33] Y. Chen, G. Parziale, E. Diaz-Santana, and A. K. Jain, "3D touchless fingerprints: Compatibility with legacy rolled images," in *Proc. Biometrics Symp., Special Session Res. Biometric Consortium Conf.*, Sep./Aug. 2006, pp. 1–6.
[34] Y. Wang, L. G. Hassebrook, and D. L. Lau, "Data acquisition and processing of 3-D fingerprints," *IEEE Trans. Inf. Forensics Security*, vol. 5, no. 4, pp. 750–760, Dec. 2010.
[35] L. Sweeney, V. Weedn, and R. Gross, "HandShot: A fast 3-D imaging system for capturing fingerprints, palm prints and hand geometry," Pittsburgh, PA, USA, Tech. Rep. CMU-ISRI-05-105, 2004.
[36] G. Parziale, E. Diaz-Santana, and R. Hauke, "The surround imagertm: A multi-camera touchless device to acquire 3D rolled-equivalent fingerprints," in *Advances in Biometrics*. Berlin, Germany: Springer, 2005, pp. 244–250.
[37] S. Malassiotis, N. Aifanti, and M. G. Strintzis, "Personal authentication using 3-D finger geometry," *IEEE Trans. Inf. Forensics Security*, vol. 1, no. 1, pp. 12–21, Mar. 2006.
[38] F. Chen, "3D fingerprint and palm print data model and capture devices using multi structured lights and cameras," U.S. Patent 7 609 865 B2, Oct. 27, 2009.
[39] C. H. Esteban and F. Schmitt, "Multi-stereo 3D object reconstruction," in *Proc. 1st Int. Symp. 3D Data Process. Vis. Transmiss.*, Jun. 2002, pp. 159–166.
[40] M. Pollefeys, D. Nistér, J.-M. Frahm, A. Akbarzadeh, P. Mordohai, B. Clipp, C. Engels, D. Gallup, S.-J. Kim, P. Merrell, C. Salmi, S. Sinha, B. Talton, L. Wang, Q. Yang, H. Stewénius, R. Yang, G. Welch, and H. Towles, "Detailed real-time urban 3D reconstruction from video," *Int. J. Comput. Vis.*, vol. 78, no. 2, pp. 143–167, Jul. 2008.
[41] D. L. Woodard, T. C. Faltemier, P. Yan, P. J. Flynn, and K. W. Bowyer, "A comparison of 3D biometric modalities," in *Proc. Conf. Comput. Vis. Pattern Recognit. Workshop (CVPRW)*, Jun. 2006, p. 57.
[42] J. N. Bradley, C. M. Brislawn, and T. Hopper, "FBI wavelet/scalar quantization standard for gray-scale fingerprint image compression," *Proc. SPIE*, vol. 1961, pp. 293–304, Aug. 1993.
[43] A. Fatehpuria, D. L. Lau, and L. G. Hassebrook, "Acquiring a 2D rolled equivalent fingerprint image from a non-contact 3D finger scan," *Proc. SPIE*, vol. 6202, Apr. 2006, Art. no. 62020C.
[44] F. Liu and D. Zhang, "3D fingerprint reconstruction system using feature correspondences and prior estimated finger model," *Pattern Recognit.*, vol. 47, pp. 178–193, Jan. 2014.

[45] S. J. Xie, J. Yang, S. Yoon, D. Park, and J. Shin, "Fingerprint quality analysis and estimation for fingerprint matching," in *State Art Biometrics*. Vienna, Austria: Intech, 2011, pp. 953–978.
[46] C. S. Mlambo and Y. Moolla, "Complexity and distortion analysis on methods for unrolling 3D to 2D fingerprints," in *Proc. 11th Int. Conf. Signal-Image Technol. Internet-Based Syst. (SITIS)*, Nov. 2015, pp. 103–109.
[47] Y. Wang, D. L. Lau, and L. G. Hassebrook, "Fit-sphere unwrapping and performance analysis of 3D fingerprints," *Appl. Opt.*, vol. 49, pp. 592–600, Feb. 2010.
[48] G. Abramovich, K. Harding, S. Manickam, J. Czechowski, V. Paruchuru, R. Tait, C. Nafis, and A. Vemury, "Mobile, contactless, single-shot, fingerprint capture system," *Proc. SPIE*, vol. 7667, Apr. 2010, Art. no. 766708.
[49] Q. Zhao, A. Jain, and G. Abramovich, "3D to 2D fingerprints: Unrolling and distortion correction," in *Proc. Int. Joint Conf. Biometrics (IJCB)*, Oct. 2011, pp. 1–8.
[50] S. Shafaei, T. Inanc, and L. G. Hassebrook, "A new approach to unwrap a 3-D fingerprint to a 2-D rolled equivalent fingerprint," in *Proc. IEEE 3rd Int. Conf. Biometrics, Theory, Appl., Syst.*, Sep. 2009, pp. 1–5.
[51] S. Rajeev, S. K. K M, and S. S. Agaian, "Method for modeling post-mortem biometric 3D fingerprints," *Proc. SPIE*, vol. 9869, May 2016, Art. no. 98690S.
[52] S. P. Rao, K. Panetta, and S. S. Agaian, "A novel method for rotation invariant palm print image stitching," *Proc. SPIE*, vol. 10221, May 2017, Art. no. 102210N.
[53] R. Rajendran, S. P. Rao, K. Panetta, and S. S. Agaian, "Adaptive alpha-trimmed correlation based underwater image stitching," in *Proc. IEEE Int. Symp. Technol. Homeland Secur. (HST)*, Apr. 2017, pp. 1–7.
[54] S. P. Rao, R. Rajendran, S. S. Agaian, and M. M. A. Mulawka, "Alpha trimmed correlation for touchless finger image mosaicing," *Proc. SPIE*, vol. 9869, May 2016, Art. no. 98690U.
[55] R. Hess and T. Roosendaal, *The Essential Blender—Guide to 3D Creation With the Open Source Suite Blender*. San Francisco, CA, USA: No Starch Press, 2007.
[56] T. Igarashi and D. Cosgrove, "Adaptive unwrapping for interactive texture painting," in *Proc. Symp. Interact. 3D Graph.*, 2001, pp. 209–216.
[57] K. C. Finney, *3D Game Programming All in One*. Boston, MA, USA: Cengage, 2013.
[58] H. Guan, B. Stanton, A. Dienstfrey, and M. Theofanos, "A measurement metric for forensic latent fingerprint preprocessing," U.S. Dept. Commerce, Nat. Inst. Standards Technol., Gaithersburg, MD, USA, 2014.
[59] S. Rajeev, S. K. K M, K. Panetta, and S. S. Agaian, "3-D palmprint modeling for biometric verification," in *Proc. IEEE Int. Symp. Technol. Homeland Secur.*, Waltham, MA, USA, Apr. 2017, pp. 1–6.
[60] R. D. Labati, A. Genovese, V. Piuri, and F. Scotti, "Touchless fingerprint biometrics: A survey on 2D and 3D technologies," *J. Internet Technol.*, vol. 15, no. 3, pp. 325–332, 2014.
[61] S. Rajeev, S. K. K M, K. Panetta, and S. S. Agaian, "Forensic print extraction using 3D technology and its processing," *Proc. SPIE*, vol. 10221, May 2017, Art. no. 102210L.
[62] (2017). *FlashScan3D | The 3D Fingerprinting Company*. [Online]. Available: http://flashscan3d.com/
[63] L. Hassebrook. *MAT5 Data Format*. Accessed: Jun. 5, 2014. [Online]. Available: http://www.engr.uky.edu/~lgh/soft/softmat5format.htm
[64] D. Popescu, F. Popister, S. Popescu, C. Neamtu, and M. Gurzau, "Direct toolpath generation based on graph theory for milling roughing," *Procedia CIRP*, vol. 25, pp. 75–80, Jan. 2014.
[65] Z. Wang, A. C. Bovik, H. R. Sheikh, and E. P. Simoncelli, "Image quality assessment: From error visibility to structural similarity," *IEEE Trans. Image Process.*, vol. 13, no. 4, pp. 600–612, Apr. 2004.
[66] S. S. Agaian, K. Panetta, and A. M. Grigoryan, "Transform-based image enhancement algorithms with performance measure," *IEEE Trans. Image Process.*, vol. 10, no. 3, pp. 367–382, Mar. 2001.
[67] S. S. Agaian, K. Panetta, and A. M. Grigoryan, "A new measure of image enhancement," in *Proc. IASTED Int. Conf. Signal Process. Commun.*, 2000, pp. 19–22.
[68] S. S. Agaian, B. Silver, and K. A. Panetta, "Transform coefficient histogram-based image enhancement algorithms using contrast entropy," *IEEE Trans. Image Process.*, vol. 16, no. 3, pp. 741–758, Mar. 2007.
[69] Y. Zhou, K. Panetta, and S. Agaian, "Human visual system based mammogram enhancement and analysis," in *Proc. 2nd Int. Conf. Image Process. Theory, Tools Appl.*, Jul. 2010, pp. 229–234.
[70] K. Panetta, Y. Zhou, S. Agaian, and H. Jia, "Nonlinear unsharp masking for mammogram enhancement," *IEEE Trans. Inf. Technol. Biomed.*, vol. 15, no. 6, pp. 918–928, Nov. 2011.
[71] K. Panetta, C. Gao, and S. Agaian, "No reference color image contrast and quality measures," *IEEE Trans. Consum. Electron.*, vol. 59, no. 3, pp. 643–651, Aug. 2013.
[72] (2011). *Development of NFIQ 2.0 | NIST*. [Online]. Available: https://www.nist.gov/services-resources/software/development-nfiq-20
[73] (2014). *Fingerprint Minutiae Viewer (FpMV) | NIST*. [Online]. Available: https://www.nist.gov/services-resources/software/fingerprint-minutiae-viewer-fpmv
[74] (2010). *NIST Biometric Image Software (NBIS) | NIST*. [Online]. Available: https://www.nist.gov/services-resources/software/nist-biometric-image-software-nbis

KAREN PANETTA (S'84–M'85–SM'95–F'08) received the B.S. degree in computer engineering from Boston University, Boston, MA, USA, and the M.S. and Ph.D. degrees in electrical engineering from Northeastern University, Boston. She is currently the Dean of Graduate Engineering Education, a Professor with the Department of Electrical and Computer Engineering, and an Adjunct Professor of computer science with Tufts University, Medford, MA, USA, and the Director of the Dr. Panetta's Vision and Sensing System Laboratory. Her research focuses on developing efficient algorithms for simulation, modeling, signal, and image processing for biomedical and security applications. She is also the President-Elect of the IEEE-HKN. She is also the Editor-in-Chief of the *IEEE Women in Engineering Magazine*. She was the IEEE-USA Vice-President of Communications and Public Affairs. From 2007 to 2009, she served as the world-wide Director for IEEE Women in Engineering, overseeing the world's largest professional organization supporting women in engineering and science. She was a recipient of the 2012 IEEE Ethical Practices Award and the Harriet B. Rigas Award for Outstanding Educator. In 2011, she received the Presidential Award for Engineering and Science Education and Mentoring by the U.S. President, Barack Obama.

SRIJITH RAJEEV received the B.E. degree in electronics and communication engineering from Visvesvaraya Technological University, India, in 2014, and the M.S degree in electrical and computer engineering from The University of Texas at San Antonio, USA, in 2016. He is currently pursuing the Ph.D. degree in electrical and computer engineering with Tufts University, USA. His current research interests include signal/image processing, video processing, deep-learning, 3D sensors and modeling, digital forensic, and biomedical applications.

K. M. SHREYAS KAMATH received the bachelor's degree (B.E.) in electronics and communication engineering from Visvesvaraya Technological University, Belgaum, India, in 2014, and the master's degree in electronic and computer engineering from The University of Texas at San Antonio, USA. He is currently pursuing the Ph.D. degree in electrical and computer engineering with Tufts University, USA. He is also a Graduate Research Assistant with the Visual and Sensing Lab, Tufts. His main research interests include the areas of signal/image processing, 3D scanning, and automated biometric technologies particularly focusing on fingerprints and their applications.

SOS S. AGAIAN is currently a Distinguished Professor with The City University of New York/CSI. His research interests include computational vision and machine learning, large-scale data analytic analytics, multi-modal data fusion, biologically inspired signal/image processing modeling, multimodal biometric and digital forensics, 3D imaging sensors, information processing and security, and biomedical and health informatics. He has authored more than 650 technical articles and ten books in these areas. He is also listed as a co-inventor on 44 patents/disclosures. The technologies that he invented have been adopted by multiple institutions, including the U.S. Government, and commercialized by industry. He is also a Fellow of the SPIE, the IS&T, and the AAAS. He also serves as a Foreign Member of the Armenian National Academy. He is also an Editorial Board Member for the *Journal of Pattern Recognition and Image Analysis*. He received the MAEStro Educator of the Year, sponsored by the Society of Mexican American Engineers. He also received the Distinguished Research Award at The University of Texas at San Antonio. He was a recipient of the Innovator of the Year Award, in 2014, of the Tech Flash Titans-Top Researcher-Award (San Antonio Business Journal, 2014), the Entrepreneurship Award (UTSA-2013 and 2016), and the Excellence in Teaching Award, in 2015. He is also an Associate Editor for several journals, including the IEEE TRANSACTIONS ON IMAGE PROCESSING, IEEE TRANSACTIONS ON SYSTEMS, MAN, AND CYBERNETICS, *Journal of Electrical and Computer Engineering* (Hindawi Publishing Corporation), *International Journal of Digital Multimedia Broadcasting* (Hindawi Publishing Corporation), and *Journal of Electronic Imaging* (SPIE, IS&T).